Journal of Pharmacy and Pharmacology, 2025, **00**, 1–16
https://doi.org/10.1093/jpp/rgaf110
Advance access publication 11 November 2025
Research Paper

JPP Journal of Pharmacy and Pharmacology

OXFORD

Molecular mechanisms involved in the immunomodulatory action of *Baccharis dracunculifolia* DC. extract using an integrated *in silico/in vitro* approach

Giorgio Cappellucci[1], Marco Biagi[2], Mariana Romão-Veiga[3,*], Vanessa Rocha Ribeiro-Vasques[3], Elisabetta Miraldi[1], Giulia Baini[1,*], José Maurício Sforcin[3]

[1]Department of Physical Sciences, Earth and Environment, University of Siena, Strada Laterina 8, Siena 53100, Italy
[2]Department of Food and Drug, University of Parma, Parco Area delle Scienze 27/A, Parma 43124, Italy
[3]São Paulo State University (UNESP), Department of Genetics, Microbiology and Immunology, Institute of Biosciences, Campus Botucatu, Dr. Plinio Pinto e Silva street, s/n, Rubião Júnior, Botucatu, SP 18618-691, Brazil
*Corresponding author. Department of Physical Sciences, Earth and Environment, University of Siena, Strada Laterina 8, Siena 53100, Italy.
E-mail: giulia.baini2@unisi.it

Abstract

Objectives: Ethnobotany and the traditional use of medicinal plants is still a key starting point for the discovery of new drugs in modern medicine, despite often being underrated. *Baccharis dracunculifolia* DC., the major source of green propolis, has been traditionally used in South America for the treatment of malaria and parasitic infections, and for liver and gastric disorders. To investigate the molecular mechanisms involved in its immunomodulatory action, an integrated *in silico/in vitro* model was developed and validated.

Methods: The phytochemical profile of a hydro-ethanolic dry extract of *B. dracunculifolia* was investigated through UV–vis and HPLC-DAD methods and implemented with LOTUS database. Through simulated digestion and computational approaches, such as Network Pharmacology, pharmacokinetics, and biological targets were predicted. To validate bioinformatic predictions and to assess the immunomodulatory potential of *B. dracunculifolia* extract, *in vitro* tests were conducted on human monocytes (THP-1) and on peripheral blood mononuclear cells (PBMC) through ELISA dosage and flow cytometry.

Key findings: Terpenoids resulted the most enriched class in Baccharis dracunculifolia extract (BDE) (>25% w/w), followed by phenolics compounds (>15% w/w) which also included artepillin C, caffeic acid derivatives, pinocembrin, and pinobanksin. With the exception of pinocembrin, most of BDE constituents displayed a limited bioaccessibility rate. MAPK, NF-κB, several cytokines and TLR-4 were identified as key targets. These predictions were experimentally validated, as *B. dracunculifolia* extract, particularly 25 μg/ml, showed to upregulate MAPK ERK1/2 and p38 activation, to modulate NF-κB and to modulate cytokine release, particularly in PBMCs, where IL-1β, IL-10, IL-6, and IL-2 increased by 27%, 39%, 17%, and 21% vs control, respectively, under basal conditions, while in the inflammatory model, it caused a selective 59% reduction in Tumor necrosis factor alpha (TNF-α) vs lipopolysaccharide (LPS). This approach provided valuable guidance for experiments while reducing both cost and time.

Conclusions: Our findings demonstrated that the integrated in silico/in vitro approach proved to be a valuable and cost- and time-efficient tool for studying *B. dracunculifolia* extract, which was shown to exert immunomodulatory activity by modulating multiple signaling pathways at both upstream and downstream levels.

Keywords: *Baccharis dracunculifolia*; chemical analysis; immune cells

Introduction

Baccharis dracunculifolia DC. (Asteraceae) is a shrubby plant belonging to the *Baccharis* genus, which is a typical genus native to South America, particularly Brazil, but can also be found in some areas of Argentina and Paraguay [1, 2].

Its shrubby shape and hard-wearing wood have led its use in the production of domestic and agricultural tools. Its popular names, "vassoura" or "vassourinha", refer to its use in making rustic brooms. The ethnobotany of this important plant, which has contributed to the survival of numerous South American communities, is well known and adequately described in literature. It has traditionally been used to treat malaria and parasitic infections. In many communities in Latin America, particularly in Brazil, tea made from the leaves and flowers has been consumed to treat liver and gastric diseases, and to alleviate inflammatory conditions [3]. *B. dracunculifolia* has also been used in religious rituals, especially in the communities in the Brazilian states of Bahia and São Paulo.

This species is adapted to open environments such as meadows and forest edges. It can grow to more than three meters in height. It has lanceolate leaves (from which the name "dracunculifolia" is derived), a dark green color and moderately coriaceous leaves. Its small yellowish-white flowers are arranged in capitular inflorescences that mainly bloom during the summer. It can tolerate different climatic conditions and reproduces easily through its numerous seeds, which can germinate when the conditions are favorable. However, it tends to be attacked by fungi when growing in very humid environments [3, 4].

B. dracunculifolia is an aromatic plant and. Among its abundant essential oils, there is a complex terpenoid structure containing oxygenated sesquiterpenes such as nerolidol and sphatulenol, as well as hydrocarbons such as

Received 24 April 2025; accepted 21 October 2025

germacrene and bicyclogermacrene. The abundant phenolic fraction contains cinnamic acid derivatives, and chlorogenic acid. The most characteristic compounds of this species are prenylated derivatives, such as 3,5-diprenyl-*p*-coumaric acid or artepillin C, 3-prenyl-4-dihydrocinnamoyloxy-cinnamic acid (baccarin), baccarin-5′-aldehyde and 3-prenyl-*p*-coumaric acid (drupanin). *B. dracunculifolia* has a high and heterogeneous flavonoids content. Several studies reported the presence of naringenin, kaempferol and its derivatives, apigenin, pinocembrin, pinobanksin, chrysin, and galangin. Furthermore, recent studies have been identified and named new glycosides, dracunculifosides A–J, which are found in the aerial parts of this plant [1, 4].

B. dracunculifolia is considered the main source of a natural resinous product made by honeybees (*Apis mellifera*), known as "green propolis", which has been widely used for medicinal purposes. Due to its rapid vegetative growth, it is often used to restore deforested areas. It is also kas a "nurturing species" because it helps other plant species to grow nearby. Despite its ethnopharmacological relevance and well-known association with green propolis, the biological potential of *B. dracunculifolia* remains largely unexplored at the molecular level. Previous studies have focused mainly on the characterization of isolated compounds or general pharmacological activities, but lacking in pharmacokinetic investigations as well as in mechanistic confirmation. This leaves a critical gap in understanding how a chemically complex matrix such as *B. dracunculifolia* interacts with specific molecular targets and signaling pathways, particularly in the context of the immune response. Although some evidence suggests immunomodulatory properties, further research is needed to clarify its impact on immune cells. To bridge this gap, the present study applies an integrated *in silico/in vitro* approach, based on pharmacokinetic and network pharmacology predictions combined with experimental testing, to describe the molecular mechanisms involved in the immunomodulatory action of *B. dracunculifolia*, evaluating the expression of Toll-like receptors (TLR-2 and TLR-4), intracellular signaling pathways (p38, MAPK, and NF-κB), and cytokine production (IL-6, TNF-α, IL-8, IL-1β, IL-2, and IL-10).

Material and methods

Plant material

The dry leaf extract of *B. dracunculifolia* was provided by Prof. Dr Jairo Kenupp Bastos, FCFRP, USP, Brazil, and was obtained by drying the leaves in an air circulation oven at 40°C before grinding them in a knife mill. The material was extracted in 70% ethanol (EtOH) by maceration, with the procedure repeated 4 times at 48 h intervals. The extract was then filtered and concentrated under vacuum in a rotoevaporator to obtain a pellet, which was subsequently freeze-dried. This was then solubilized in 70% (w/w) EtOH (BDE) to obtain 50 mg/ml, which was then diluted as required for chemical and biological assays.

Quantification of total polyphenols and flavonoids content

The total polyphenol content was quantified by the Folin–Ciocalteu colorimetric assay [5], with a 70% BDE ethanolic solution at a concentration of 10 mg/ml. Absorbances were measured spectrophotometrically (UV/Vis spectrophotometer UV-1900i, Shimadzu, Japan) at 700 nm, with a blank consisting of EtOH reacted under the same conditions. The calibration line was performed using gallic acid, with a $R^2 > 0.99$ and a limit of quantification of the assay (LOQ) < 1 μg. The polyphenol concentration in the samples was calculated as percentage (%) w/w expressed as gallic acid equivalent (GAE).

Total flavonoids were quantified according to Governa *et al.* [6], Sberna *et al.* [7] and Cappellucci *et al.* (2024) [6–8]. BDE (10 mg/ml in EtOH) was diluted 1:200 in 70% EtOH and absorbances were measured at 353 nm using a VICTOR Nivo 3S multimode plate reader (PerkinElmer, Waltham, Massachusetts, USA). Quercetin was used as a standard ($R^2 > 0.98$, LOQ of the assay <0.5 μg).

All assays were conducted in triplicate.

Total flavan-3-ols content

The presence of catechins and proanthocyanidins (total flavan-3-ols) was assessed using the vanillic aldehyde assay. For this, an aliquot was taken and added to 1 ml of 11.5 N hydrochloric acid and 0.5 ml of a 1% vanillin solution in EtOH. In an acidic medium, the catechin A ring reacts with vanillic aldehyde to form a red adduct, with an absorption maximum at 500 nm. The assay is positive if the red color appears immediately. Pure catechin was used as a positive control ($R^2 > 0.99$, LOQ of the assay <2 μg [9, 10]).

Triterpene content

Total triterpene quantification was performed according to Pedrosa *et al.* [11] [11]. First, 250 μl of a 5% vanillin in glacial acetic acid solution and 500 μl of sulphuric acid (99.5%) were added to 75 μl of BDE in 70% EtOH solution, in this order. Then, the solution was kept in a water bath (60 ± 1°C) for 30 min and then transferred to an ice bath adding 2500 μl of acetic acid (99.7%). The resulting solution was kept under cooling for 20 min, followed by a further 20 min at room temperature. For the negative control, 75 μl of water was used and subjected to the same assay.

Quantification was performed using a standard curve obtained with a β-sitosterol solution ($R^2 > 0.97$, LOQ of the assay <10 μg). Absorbances were read at 548 nm using a VICTOR Nivo 3S multimode plate reader (PerkinElmer, USA).

Polysaccharide content

Samples (20 μl) were diluted in 380 μl of ultrapure water and placed in a reaction tube. Then, 200 μl of a 6% w/v aqueous phenol solution were added. Next, 0.5 ml of 98% m/m sulfuric acid was added and the reaction tube was quickly closed. After 10 min at 80°C, the absorbance was read at 490 nm using a Shimadzu UV-1900 spectrophotometer. The amount of polysaccharides was calculated by interpolating the data on the standard curve constructed using D(+)-glucose (Merck, USA) and multiplying by 0.9 to convert D(+)-glucose to polysaccharides [8] ($R^2 > 0.99$, LOQ of the assay <2.5 μg).

Chromatographic profile

High-performance liquid chromatography coupled with a diode array detector (HPLC-DAD) analysis was performed using a Shimadzu Prominence LC 2030 3D instrument (Shimadzu, Japan), equipped with a 10 mm × 300 mm, 3.9 mm i.d., 125 Å Bondapak® C18 column (Waters Corporation, USA).

The mobile phases were water solutions containing 0.1% formic acid (A) and methanol containing 0.1% formic acid (B). The applied analysis method was as follows: (B) from 40% at 0.01 min to 65% at 12.00 min, 70% at 25.00 min, 75% at 30.00 min, 85% at 35.00 min, and finally 40% at 39.00 min, before stopping at 45.00 min. The flow rate was set at 0.75 ml/min. Chromatograms were recorded at 280 nm.

The calibration curves of the standards were used to quantify the associated peaks in each sample. Artepillin C, pinocembrin, pinobanksin, and caffeic acid (Merk Sigma-Aldrich, Saint Louis, MO, USA) were used as standards. The peaks of the compounds were identified by comparing their retention times (RTs) and ultraviolet spectra with those of the corresponding standards. Calibration curves were obtained for all external standards within the range 0–5 μg, with $R^2 > 0.99$, with LOD < 0.02 μg/ml, LOQ < 0.05 μg/ml, and % recovery of internal standards in tested samples 95%–105%. Inter- and intra-day variation of mean values was < ±5% of mean values.

Three independent runs were performed.

In vitro simulated bioaccessibility assay

The test was conducted according to the validated INFOGEST protocol with few modifications [12, 13]. Briefly, 1 ml of BDE (25 mg/ml) in 70% EtOH was added to 4 ml of simulated gastric juice containing porcine gastric mucosa pepsin (300 IU/ml, Merck) and NaCl (10 mg/ml), and the pH of the solution was adjusted to 1.7 with HCl. The samples were kept under agitation and incubated for 2 h at 37°C. Then, 4 ml of a solution containing porcine pancreatin (activity equivalent to 4 × U.S.P., 10 mg/ml, Merck) and a mixture of bile salts (20 mg/ml, Merck) was added, and the pH was adjusted to 7.0 by adding $NaHCO_3$ (15 mg/ml, Merck) to simulate the intestinal environment. The samples were then filtered and immediately analyzed by HPLC-DAD. The bioaccessibility rate of each compound was calculated as the percentage of its recovery after digestion compared to the initial amount.

Three independent experiments were performed.

Computational integration of phytochemistry data

To integrate the data collected from phytochemical analyses and to identify the compounds obtained through HPLC-DAD analyses, LOTUS was used. LOTUS is an open scientific database containing over 750 000 referenced structure-organism pairs. It is hosted both on Natural Products Online, an open-source project for archiving, researching and analyzing natural products, as well as on Wikidata. The Wikidata version enables the scientific community to curate the data and add new information. It provides a highly intuitive experience, offering features such as structural searches, taxonomy-oriented queries, and the export of flat tables and structures [14]. "baccharis dracunculifolia" was entered as the input for extrapolating the <organism-molecule> data.

Computational approach for the molecular target and pharmacokinetics prediction

The computational analysis of the pharmacokinetic characteristics of BDE constituents and the prediction of possible molecular targets implicated by the latter was performed using the freely accessible software described below. The SMILES was inserted as input for SwissADME, SwissTarget and SEA or the related genes directly (Gene Recommender) of artepillin C, pinobanksin, pinocembrin, baccarin, drupanin, cinnamic acid, caffeic acid, vicenin-2, rhamnocitrin, isosakuranetin, dracunculifoside (A–I), naringenin and friedenalol. They were derived from the supplementation made with LOTUS as described above.

SwissADME© is a free platform created and developed by the Molecular Modeling Group at the Swiss Institute of Bioinformatics (SIB) for the prediction of the pharmacokinetic of various chemicals. Based on physicochemical characteristics, compound similarities and the provided data, the trained algorithm estimates compounds for ADME (absorption, distribution, metabolism, and excretion) properties, as well as their physical chemistry, drug similarity, pharmacokinetics, and medicinal chemistry properties [12, 14].

The Network Pharmacology (NP) approach to obtaining evaluations and predictions of possible molecular targets was performed using three freely available web platforms, as follows:

SwissTargetPrediction: a platform (SIB group) that provides a functionality and relevance score by matching query terms based on Tanimoto similarity calculations, which are derived from ChEMBL compound annotations [12, 15];

The SEA (Similarity Ensemble Approach) predicts the biological targets of a compound based on its similarity to ligands that are annotated in reference databases. SEA also relates proteins based on their pharmacology by aggregating the chemical similarity between entire sets of ligands [12];

Both SwissTargetPrediction and SEA perform Tanimoto similarity calculations based on compound annotations derived from ChEMBL [12];

GeneRecommender (TheProphetAI S.r.l., https://www.generecommender.com/. Accessed on 10 September 2024) is a platform that uses a proprietary neural network called DeepProphet and relies on other prediction platforms, such as GenaMANIA (http://www.genemania.org/), to obtain predictions of gene/target interactions [16]. Genes related to the previously described chemicals were obtained either directly from the GeneRecommender platform or, when not present there, from the Search Tool for Interacting Chemicals database created by Szklarczyk *et al.*, (2026) [17].

Biological analysis

THP-1 cell culture and peripheral blood mononuclear cells

THP-1 cells were cultured in 75 cm^2 flasks containing RPMI 1640 medium supplemented with 10% fetal bovine serum (FBS—Euroclone, Milan, Italy), 1% L-glutamine, 1% antibiotic solution (penicillin and streptomycin, Sigma-Aldrich) and 0.05% 2-mercaptoethanol (Sigma-ldrich). The flasks were incubated at 37°C and 5% CO_2 with daily medium changes until the cells reached a confluence of 70%. Cell counts were performed using a hemocytometer and a Leica microscope (Wetzlar, Germany) at 25× magnification [18].

PBMC were collected as previously described [19], from donors who were recruited during routine occupational health checks and who had signed an informed consent form allowing the use of biological samples only for basic research only. The PBMC were isolated using a Histopaque®-1077 (Sigma-Aldrich) density gradient centrifugation process. The PBMC layer was collected, washed, and suspended in RPMI 1460 medium supplemented with 1% L-glutamine and 1% penicillin/streptomycin. Cell counting and viability were performed using a hemocytometer and trypan blue staining.

BDE (at concentrations of 1, 5, 10, 25, 50, and 100 μg/ml) was added and cells were incubated for 24 h with RPMI 1640 medium supplemented with antibiotics, glutamine and 3% FBS. To investigate the effects of BDE on cell viability, the expression of cellular markers and cytokine production, the cells were incubated with increasing concentrations of BDE for 24 h. These concentrations were selected because they are suitable for *in vitro* studies with natural products, and to assess the immunological effects, starting from 1 μg/ml (sub-physiological) up to high concentrations (100 μg/ml) to assess the maximal effect of BDE even at concentrations above physiologically relevant levels *in vitro*.

Time points were chosen to assess rapid (6 h or 15 min) and late (24 h or 60 min) immune activation. This temporal approach enables a more comprehensive evaluation of the BDE immune activity dynamics.

THP-1 cells viability

All cytofluorimetric analyses were conducted on THP-1 cells (1×10^5/ml) seeded in 24-well plates and incubated with RPMI 1640 supplemented with antibiotics, glutamine and 10% FBS at 37°C and 5% CO_2 for 24 h prior to treatments. Then, BDE (1, 5, 10, 25, 50, and 100 μg/ml) was added and cells were incubated for 24 h with RPMI 1640 supplemented with antibiotics, glutamine and 3% FBS. After incubation, cells were collected, placed in cytometry tubes, centrifuged and washed in PBS (1×). For annexin binding, the buffered solution was used and 0.5 μg of annexin V and 0.35 mg of propidium iodide (PI) were added. The cells were then incubated for 15 min at 20°C and analyzed using the FACSCanto™ flow cytometer. At least 20 000 events were recorded for each analysis, which was performed independently at least three times. Data were analyzed using a CFlow Plus software (BD Biosciences, USA) [20].

TLR-2 and TLR-4 expression

After treating THP-1 cells with BDE (1, 5, 10, 25, 50, and 100 μg/ml), the expression of TLR-2 and TLR-4 was determined by flow cytometry. After 24 h, cells were incubated for 20 min in the dark at 4°C, with monoclonal antibodies and respective fluorochromes: anti-TLR2 (PE) and anti-TLR4 (FITC) (BD Biosciences, USA). After centrifugation, cells were washed twice with phosphate-buffered saline (PBS) containing 0.5% bovine serum albumin and centrifuged for 5 min at 200 g. The cells were fixed with buffered saline containing 2% paraformaldehyde in PBS (BD Biosciences). Control tubes were incubated with specific isotypic antibodies for each fluorochrome (PE and FITC) for each test performed. Samples were acquired from 50 000 events using a FACSCanto™ II flow cytometer (BD Biosciences) with FACSDIVA software (BD Biosciences). The results were analyzed using FlowJo software, version X.10.6 (FlowJo, LLC, Three Stars Inc., Ashland, OR, USA), and results were plotted as the median fluorescence intensity (MFI) of cells expressing the marker [21].

All tests were conducted in triplicate.

Evaluation of intracellular signaling pathways

After treating and incubating THP-1 cells with BDE (10 and 25 μg/ml) for 15 and 60 min, the cells were adjusted to 2×10^5 cells/ml and aliquots were transferred to Falcon cytometer tubes (Corning Incorporated, NY, USA). After centrifugation, the cells were washed with a wash buffer (BD Biosciences), fixed using cytofix (BD Biosciences) and permeabilized using Perm III (BD Biosciences). After, cells were incubated for 30 min in the dark and at room temperature with fluorochrome-labelled antibodies against the following intracellular proteins: anti-phospho-p65-NF-κB (PE-Cy7), anti-phospho-p38MAPK (PE-Cy7), anti-phospho-ERK1/2 (PE-Cy7) and anti phospho-NF-kB (p65). To define the gates, a control tube was incubated with a specific isotypic antibody for the PE-Cy7 fluorochrome in each test. Samples were acquired from 50 000 events using a FACSCanto™ II flow cytometer (BD Biosciences) with FACSDIVA software (BD Biosciences). The results were analyzed using FlowJo software, version X.10.6 (FlowJo, LLC, Three Stars Inc., USA), and results were plotted as the percentage (%) of cells expressing the markers [22].

Cytokine production

For cytokine quantitation, PBMC and THP-1 cells (1×10^6/ml) were placed in 24-well plates. PBMC were treated immediately with BDE, while THP-1 cells were incubated at 37°C and 5% CO_2 for 24 h prior to treatment. Both cell lines were treated with BDE (10, 25, and 100 μg/ml) under basal conditions or were co-stimulated with LPS (100 ng/ml, Sigma-Aldrich), which was used as a positive control. The cells were then incubated for 6 and 24 h, with an additional 2 h incubation period for THP-1 cells to assess a rapid TNF-α production. Assays were performed in triplicate in three independent trials. Control cells were incubated with RPMI 1640 only.

Cytokines were assayed using ELISA kits (Thermo Fisher Scientific Inc., USA), according to the manufacturer's instructions. The following cytokines were assayed: TNF-α (88–7346-22), IL-1β (88–7621-22), IL-6 (88–7066-22), IL-8 (88–8086-22), IL-2 (88–7025-22), and IL-10 (88–7016-22).

Statistical analysis

A one-way analysis of variance (ANOVA) followed by Tukey's post-hoc test was used to compare the datasets and assess the statistical significance ($P < 0.05$). Data are presented as means ± standard deviation (SD). The analyses were conducted using SPSS for Windows® v.25 (SPSS Inc., Chicago, IL, USA) and Graphpad Prism (San Diego, CA, USA).

Results

BDE phytochemical characterization

Colorimetric analyses showed that the two predominant chemical families found in BDE were terpenoids and phenolics compounds (25.27 and 15.41%, respectively) (Table 1). As to the phenolic fraction, the abundant presence of cinnamic acid derivatives was quantified at 8.04% (w/w), including caffeic acid and the main peak, which is likely to be an isomer of ferulic acid, in accordance with literature data [23]. Artepillin C, undoubtedly the most characteristic constituent of the *Baccharis* genus and Brazilian green propolis, was detected with a RT of 24.75 min and quantified at 0.41% (w/w). Interestingly, two compounds that are more typically found in European propolis, pinocembrin and pinobanksin, were also present at concentrations of 0.22% and 0.57% (w/w), respectively [6]. The polysaccharide fraction was also very high (around 12% w/w) (Table 1; Fig. 1; Table 2).

Table 1. Chemical composition of BDE.

Chemical group	Total content % (w/w)
Polyphenols	15.41 ± 1.12
Flavonoids	6.43 ± 0.46
Polysaccharides	11.63 ± 0.24
Triterpenes	25.27 ± 0.23
Flavan-3-ols	1.51 ± 0.12

Simulated bioavailability

Although the presence of bile salts and digestive enzymes affected the chromatogram of post-digested BDE, all the compounds previously identified by HPLC-DAD in the undigested BDE could still be detected, albeit with different stability percentages (Fig. 2). Specifically, as seen in Table 3, cinnamic acid derivatives were found to be stable within a range of ∼2% (ferulic acid derivative) to 15%. Caffeic acid was found to be the most stable component. Artepillin C also exhibited a low bioaccessibility rate (around 6%). The difference in stability between pinobanksin and pinocembrin, ∼10 and 80% respectively, is interesting and is most likely dependent on the hydroxyl group present on the C3 of pinobanksin.

These results demonstrate that the amount of active ingredient actually available for absorption in a physiological context can be significantly lower than the initial concentration present in the extract. In this context, being aware of the low total bioaccessibility rate of BDE constituents, we used different concentrations in *in vitro* assays starting from 10 mg/ml, covering a broad spectrum of exposure conditions.

Lotus

Using LOTUS by entering "baccharis dracunculifolia" as input allowed the evaluation of 275 molecules identified to date within the species and entered by the scientific community in wikidata. Phytochemical investigations revealed that most of these molecules belonged to the terpenoid family. In addition to these molecules, cinnamic acid derivatives and flavonoids stood out. Of the 275 molecules, those that were most described in the scientific literature [1, 4, 24] and could not be identified using HPLC were selected as the input for NP predictions, namely drupanin, rhamnocitrin, isosakuranetin, naringenin and the dracunculiphosides A to I (Fig. 3).

Integrating the molecules identified by LOTUS with those identified by HPLC-DAD analysis and adding baccharin, vicenin-2 and freidenalol—which were found in the literature but were not included in wikidata and therefore not associated with LOTUS, resulted in the inputs used for *in silico* pharmacokinetic and molecular target prediction analyses (Table 4).

In silico pharmacokinetic analyses

The molecules obtained from the integration of HPLC-DAD, literature and LOTUS analysis (Table 4) were analyzed using SwissADME® to obtain *in silico* predictions about their pharmacokinetics. Figure 4 illustrates the outputs obtained for artepillin C and pinocembrin.

As can be seen in Table 5, only drupanin, naringenin and vicenin-2 were the only substrates of P-glycoprotein (P-gp) identified. Similarly, dracunculifosides A, B, C, and D were also substrates, unlike the others, which did not appear to interact with any of the indicated cytochromes.

Figure 5, based on the boiled-egg model, shows that all molecules except for the dracunculiphosides and friedenalol had a good potential for absorption by the intestinal epithelium. Interestingly, there is a certain correspondence with the simulated digestion data for pinocembrin and pinobanksin: pinocembrin also appears to be more likely to be absorbed, enabling it to pass the blood–brain barrier (BBB) and highlighting its increased bioavailable. Naringenin was found to be the only P-gp substrate molecule capable of being absorbed in the gut.

Investigation of NP and prediction of molecular targets

NP was used to identify shared immune targets of all the molecules that could be inserted as input to obtain multiple shared genes. Despite the low combined scores obtained, except for some rare cases, our attention was focused mainly on the genes most shared between the molecules. This was done in consideration of the potential matrix effect of a heterogeneous phytochemical profile, such as that of BDE.

In silico analyses from SwissTargetPrediction revealed clear evidence of possible interactions between the molecules and genes involved in intracellular signalling pathways, including the PI3K subunits p110α, p110β and p110γ, the MAPK p38 and c-Jun, and the NF-κB inhibitory subunit IκBα. Additionally, possible interactions with several cytokines or their receptors were identified. Finally, a possible interaction with TLR-4 was obtained for one molecule only, with a high combined score of 0.92.

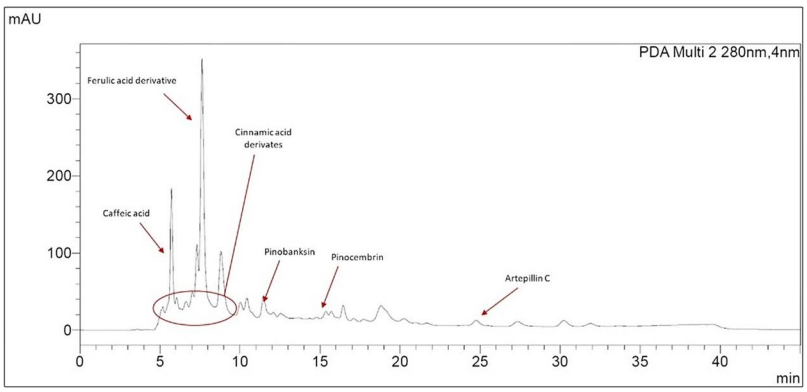

Figure 1. Chromatogram of BDE acquired at 280 nm.

Table 2. Quantification and retention time (RT) of HPLC-DAD recognized compounds.

Components	RT (min)	Total content % (w/w)
Total cinnamic acid derivatives	From 5.71 to 8.82	8.04 ± 0.17
Caffeic acid	5.72	1.56 ± 0.25
Ferulic acid derivative	7.63	4.16 ± 0.23
Pinobanksin	11.47	0.57 ± 0.08
Pinocembrin	15.37	0.22 ± 0.01
Artepillin C	24.75	0.41 ± 0.04

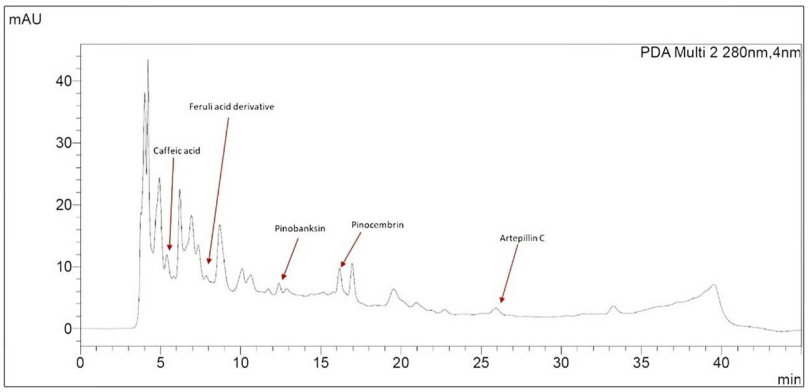

Figure 2. Chromatogram of BDE acquired at 280 nm after simulated digestion.

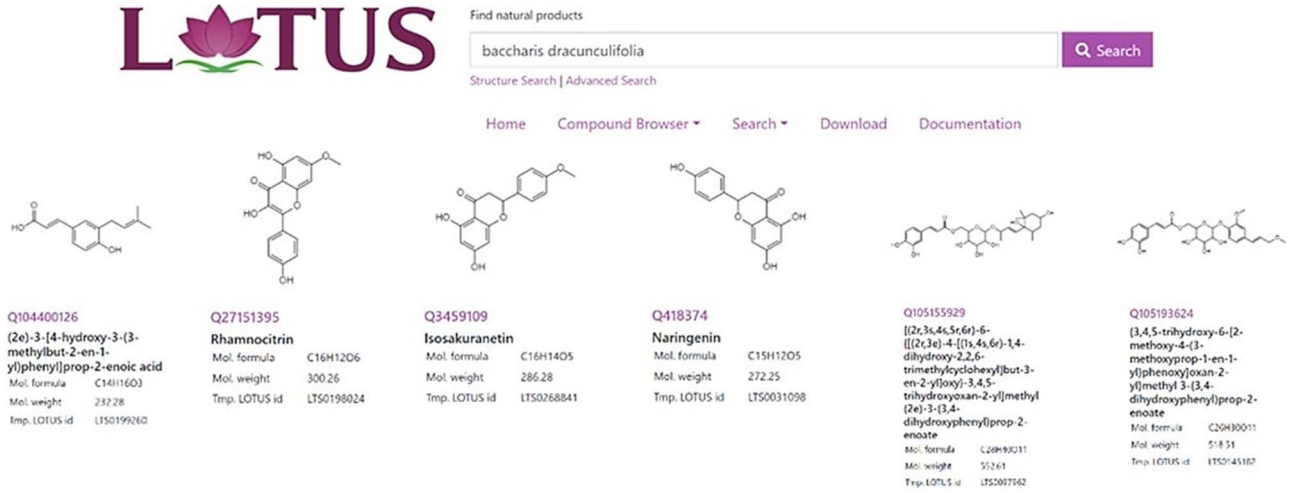

Figure 3. Drupanin, rhamnocitrin, isosakuaranetin, naringenin, dracunculiphoside A and dracunculiphoside D, highlighted by LOTUS in the <organism-molecule> correspondence.

Table 3. Quantification by HPLC-DAD of recognized compounds in BDE after simulated digestion.

Components	Remaining content % (w/w) at post digestion time
Total cinnamic acid derivatives	8.91 ± 1.41
Caffeic acid	15.19 ± 0.81
Ferulic acid derivative	2.09 ± 0.27
Pinobanksin	10.47 ± 1.32
Pinocembrin	79.48 ± 15.88
Artepillin C	5.62 ± 1.39

(Additional molecular target predictions with SwissTargetPrediction are reported in Supplementary Table S1)

SEA analysis also revealed a convergence on genes involved in cell signalling processes. These included AP-1, a transcription factor downstream of MAPK, and p105, the B-subunit of NF-κB shared by 10 molecules. IL-2 was also identified as a potential target for eight molecules, with a combined score of 0.48—also quite high compared to the others.

(Additional molecular target predictions with SEA are reported in Supplementary Table S2)

Using a third tool with slightly different functionality finally confirmed the results reported so far. In fact, inserting the genes related to the molecules in GeneRecommender and using the integrated GeneMANIA platform, same gene predictions already highlighted by SwissTargetPrediction and SEA were retrieved. Interrogating NP with GeneRecommender and applying filters to analyse genes implicated in immune system and inflammatory processes, it was noted a convergence on signalling pathways such as MAPK and NF-κB, and cytokines

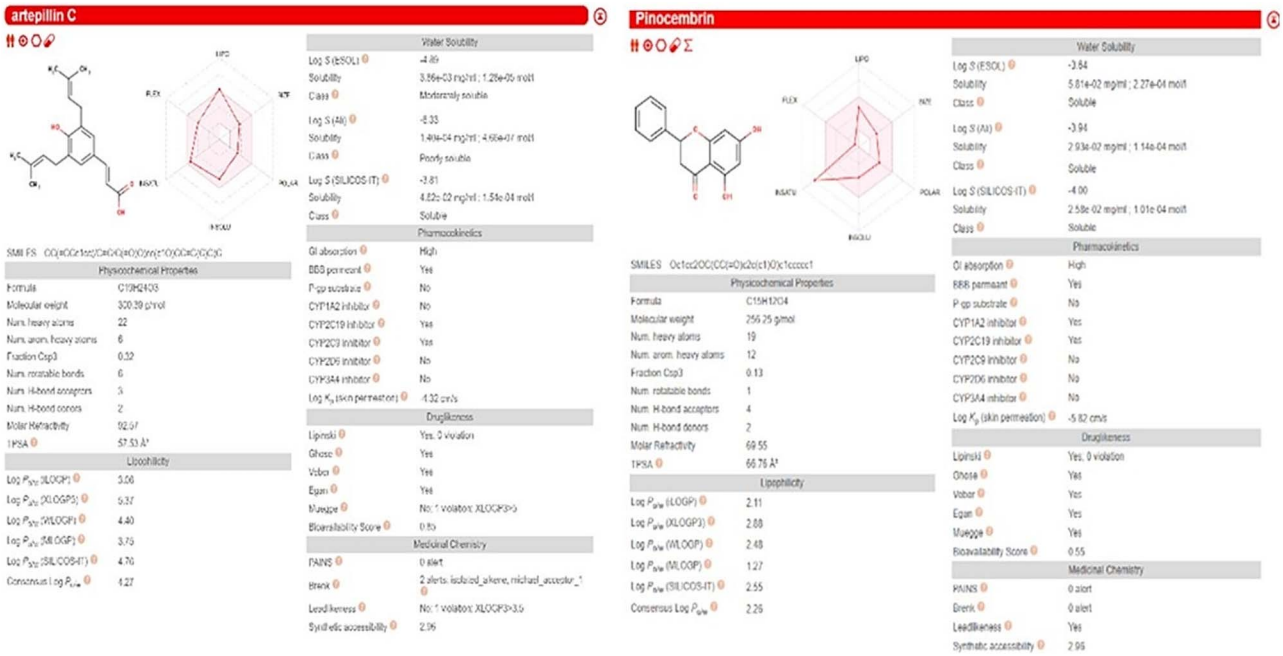

Figure 4. SwissADME-derived outputs for artepillin C and pinocembrin, from left to right.

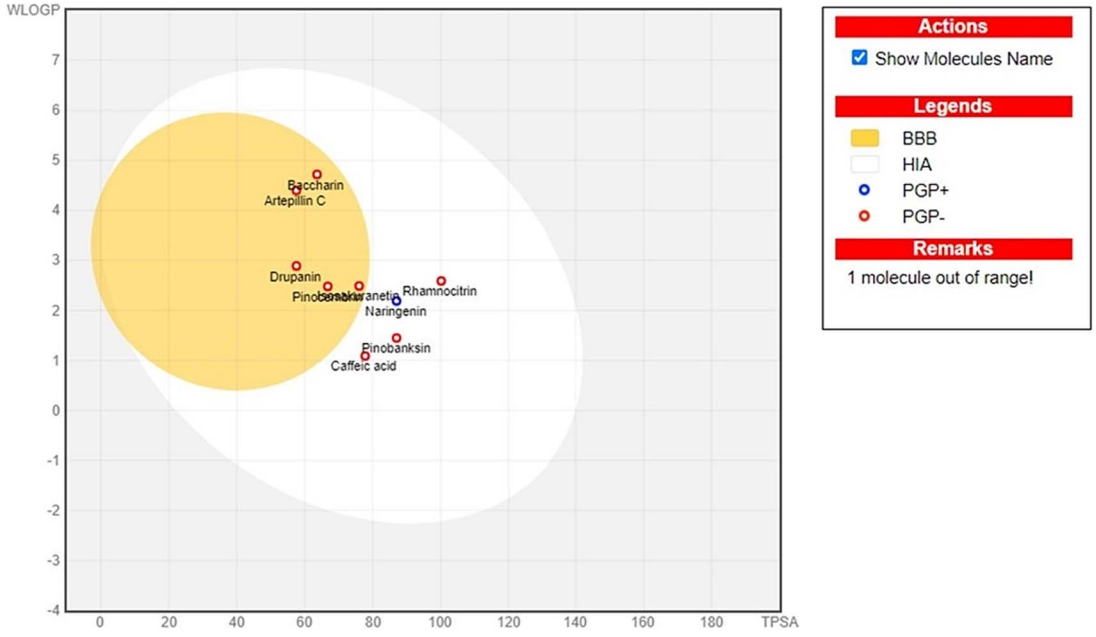

Figure 5. Predictions of absorption of all chemicals using the SwissADME boiled-egg model.

such as TNF-α, IL-6, IL-1β, IL-8 and IL-2, as well as the possible involvement of TLR-4.

These predictions obtained from three bioinformatic tools led to subsequent biological analyses, which verified the involvement of the ERK1/2, p38 and NF-κB signalling pathways as well as the TLR-4 membrane receptor; and the TNF-α, IL-1β, IL-6, IL-2 and IL-8 cytokines. The involvement of these predicted targets was assessed in *in vitro* tests. TLR-2 and IL-10 expression was also analysed to provide a more comprehensive overview, given their functional relationship with the predicted targets.

(Additional molecular target predictions with GeneRecommender are reported in Supplementary Fig. S1)

BDE exerts no cytotoxic effects on THP-1 cells

The safety of BDE on THP-1 cells was assessed before investigating the biological activities. No significant differences in cell viability were observed after incubation with BDE at any concentration. A slight increase in apoptosis, late apoptosis and necrosis after incubation with the highest concentration (100 μg/ml) indicated that none of the concentrations had a cytotoxic effect, leaving 96.2% of cells viability (see Fig. 6).

The viability of the PBMCs was evaluated by cell counting and trypan blue staining. Once >95% viability was confirmed, morphological inspections were performed at regular time points after seeding to exclude cell death.

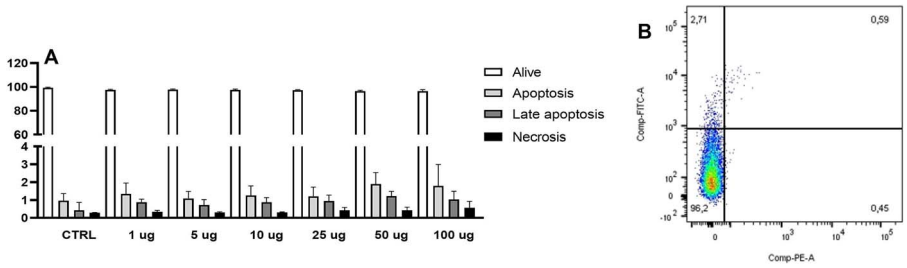

Figure 6. On the left, percentage of THP-1 cell viability (A) after incubation with BDE at the different concentrations tested. On the right, representative dotplot of BDE 100 μg/ml (B) showing live cells (96.2%), apoptotic cells (2.71%), late apoptotic (0.59%), and necrotic cells (0.45%).

Table 4. Inputs used for NP analyses obtained by cross-referencing data from phytochemical analyses, literature and LOTUS.

Chemical family	Molecules
Prenylates and cinnamic derivates	Cinnamic acid
	Artepillin C
	Baccharin
	Drupanin
	Dracunculifosides (A-I)
Flavonoids	Vicenin-2
	Rhamnocitrin
	Isosakuranetin
	Naringenin
	Pinocembrin
	Pinobanksin
Terpenoids	Friedelanol

BDE stimulated TLR-4 but not TLR-2 expression

In addition to the TLR-4 assessment predicted by SwissTarget and GeneMANIA although for a single molecule of the BDE phytocomplex but with a high combined score of 0.92 for SwisseTargetPrediction, TLR-2 was also investigated [25]. The evaluation was performed in relation to control (untreated cells) and to LPS (100 ng/ml), which is a known activator of these membrane receptors [26]. A possible effect displayed by EtOH—BDE solvent, was also evaluated. The results were in close agreement with NP's predictions. As shown in Fig. 7, TLR-2 expression increased slightly in a not significant manner with all BDE concentrations; on the other hand, TLR-4 expression increased significantly with concentrations between 5 and 100 μg/ml, with increases ranging between +46.65 and 64.96 MFI vs CTRL ($P <$ .05). EtOH 0.1% (v/v), representing the highest solvent concentration in BDE 100 μg/ml, had no effect on these parameters.

BDE activated intracellular signaling pathways

In light of the results obtained for cell viability and the minimal differences observed in the activation of TLR-2 and TLR-4 at the various tested concentrations of BDE, the signaling pathways predicted by NP were examined on THP-1 cells at two concentrations (10 and 25 μg/ml) after 15 and 60 min of treatment.

As shown in Fig. 8, BDE 10 μg/ml increased phosphorylated p38-MAPK expression after 15 min (+7.12 fold vs CTRL, $P <$ .001), but this effect was not maintained after 60 min. Similarly, BDE (25 μg/ml) increased p38 expression over time, reaching a maximum after 60 min (+55.62 fold vs CTRL, $P <$ .001). BDE increased phosphorylated ERK1/2 expression constantly after 15 and after 60 min, with maximal values obtained at a concentration of 25 μg/ml at the later time point (+58.57 fold vs CTRL, $P <$ .001). Regarding the phosphorylated form of NF-κB p65, BDE (25 μg/ml) was found to increase its expression after both 15 and, in particular, 60 min (+22.75 vs CTRL, $P <$ .001). Slight increase was also recorded for BDE 10 μg/ml but it was not statistically significant. NF-κB gene expression increased most markedly with LPS 100 ng/ml, which was used as a positive control (data not shown).

(Additional activation percentage (%) of NF-κB by LPS is reported in Supplementary Fig. S2)

Cytokine production

The effects of BDE on cytokine production by THP-1 cells were assayed using three different concentrations (10, 25 and 100 μg/ml) at baseline and following a LPS stimulus after 6 and 24 h. LPS (100 ng/ml) was used as a positive control.

IL-6, TNF-α, and IL-8 production were unaffected by BDE under basal conditions (Fig. 9).

In the inflammatory model (Fig. 10), BDE prevented LPS activity by mildly inhibiting the production of IL-6 and, in particular, TNF-α in a statistically significant manner after 6 h of treatment. In contrast, co-treatment with BDE and LPS resulted in an increased IL-8 production.

TNF-α level in basal conditions and in co-treatment with LPS was also measured reducing the treatment period to 2 h. In this protocol, BDE was devoid of activity in basal conditions (Fig. 11—above) while significant concentration-dependent downregulation of TNF-α was observed in the co-treatments: −32.41% for the 10 μg/ml, −49.44% for the 25 μg/ml and − 65.19% for the 100 μg/ml vs LPS ($P <$ .001) (Fig. 11—below).

Having evaluated the effect of BDE on THP-1 cells, we proceeded to analyse its overall impact on immune cells by determining the same cytokines using PBMC isolated from healthy volunteers. This approach enabled us to evaluate immune responses in a more comprehensive and specific manner by incorporating the role of the lymphocytic component.

Unlike THP-1 cells, dosages carried out using PBMC under basal conditions showed that BDE (25 μg/ml) significantly increased the production of IL-6 (+17%, $P <$ .05 vs CTRL), IL-2 (+21%, $P <$ .05 vs CTRL), IL-10 and IL-1β (+39% and + 27% respectively vs CTRL, $P <$ .001) after 24 h. Even if in lesser extent, IL-1β was also upregulated after 6 h (+18%, $P <$ .05 vs ctrl). Even in PBMCs, no modulation was observed for TNF-α under basal conditions. Furthermore, BDE 100 μg/ml statistically significantly increased the production of IL-1β and IL-10 after 24 h (Fig. 12).

Table 5. SwissADME predictions of interactions with P-glycoprotein (P-gp) and cytochromes.

Compounds	P-gp	CYP1A2	CYP2C19	CYP2C9	CYP2D6	CYP3A4
Artepillin C	−	−	+	+	−	−
Baccharin	−	+	+	+	−	−
Caffeic acid	−	−	−	−	−	−
Cinnamic acid	−	−	−	−	−	−
Dracunculiphoside (A, B, C, D)	+	−	−	−	−	−
Dracunculiphoside (E, F, G, H, I)	−	−	−	−	−	−
Drupanin	+	−	−	−	−	−
Friedenalol	−	−	−	−	−	−
Isosakuranetin	−	+	+	−	−	+
Naringenin	+	+	−	−	−	+
Pinobanksin	−	−	−	−	−	−
Pinocembrin	−	+	+	−	−	−
Rhamnocitrin	−	+	−	−	+	+
Vicenin-2	+	−	−	−	−	−

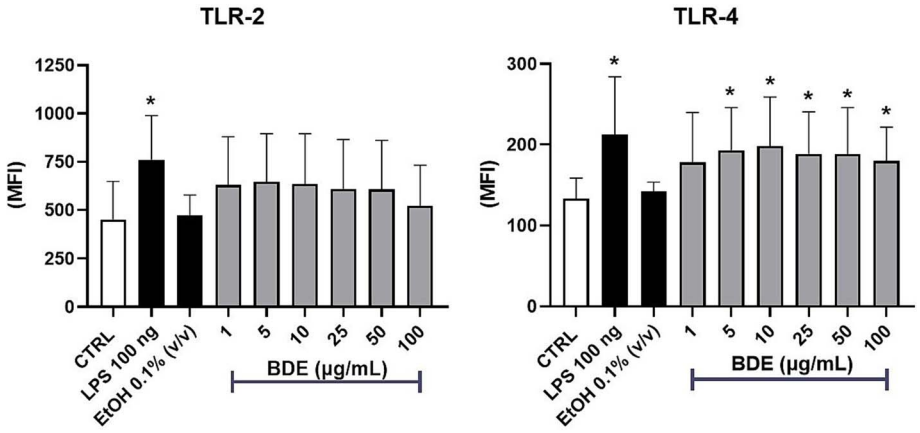

Figure 7. TLR-2 and TLR-4 median fluorescence intensity (MFI) of monocytes incubated with RPMI 1640 (control—CTRL), lipopolysaccharide (LPS—100 ng/ml), ethanol (EtOH 0.1%), or BDE (1, 5, 10, 25, 50, and 100 μg/ml) for 24 h. *$P < .05$ vs CTRL (one-way ANOVA).

In the inflammatory model (Fig. 13), a decreased TNF-α production was confirmed at 6 h, with BDE acting in a concentration-dependent manner, down-regulating this cytokine by 56%, 59% and 78% for BDE 10, 25, and 100 μg/ml respectively (vs LPS, $P < .001$). IL-10 expression also showed to be significantly reduced with BDE 10 and 25 μg/ml after 24 h, respectively −25% ($P < .001$) and −17% ($P < .01$). At 100 μg/ml BDE reduced IL-10 expression after 6 h (−33% vs LPS, $P < .001$), but upregulated this cytokine after 24 h (+40% vs LPS, $P < .001$). Also IL-2 expression was slightly downregulated, even if only at 100 μg/ml after 24 h (−16% vs LPS, $P < .05$). On the contrary, an increased production of IL-6 (after 6 and 24 h) and IL-1β (24 h) was observed with BDE 100 μg/ml vs LPS. The other two concentrations did not affect the production of these cytokines.

Discussion

Ethnobotany and the study of traditional use of medicinal plants have always been a starting point for drug discovery [27]. However, it is difficult to extrapolate information from traditional medicine and ethnobotanical studies into scientific approaches and preclinical studies. Preparations such as infusions, decoctions, and poultices made from *B. dracunculifolia* have long been used in traditional South American medicine for their anti-inflammatory properties, both systemically and topically. Also, green propolis mainly derived from this species is enriched in polyphenols and lipophilic compounds and has been reported to exert well established biological activities, including antimicrobial and immunomodulatory effects [28]. In this work, with the aim of studying for the first time *B. dracunculifolia* taking into consideration the whole phytocomplex, we extracted the herbal material using a 70% hydroethanolic solution that resulted the best solvent to balance the content of hydrophilic and lipophilic constituents, obtaining the sample analysed and tested, BDE.

This study aimed to investigate the phytochemistry and biological activity of BDE in terms of pharmacokinetics and pharmacodynamics, employing an integrated *in silico/in vitro* approach. This was made possible by the innovative equipment constantly interfaced with the NP, as well as by collaboration between different research groups.

The use of NP, especially for the study of species of ethnobotanical interest, is a modern practice that has grown in popularity in recent years as evidenced by the literature [29–31]. NP is often an indispensable aid in the scientific study of species that are traditionally used and poorly investigated. Unlike most studies evaluating medicinal plants through *in silico* computational approaches [32, 33], this specific integration with NP predictive models aims to analyse the

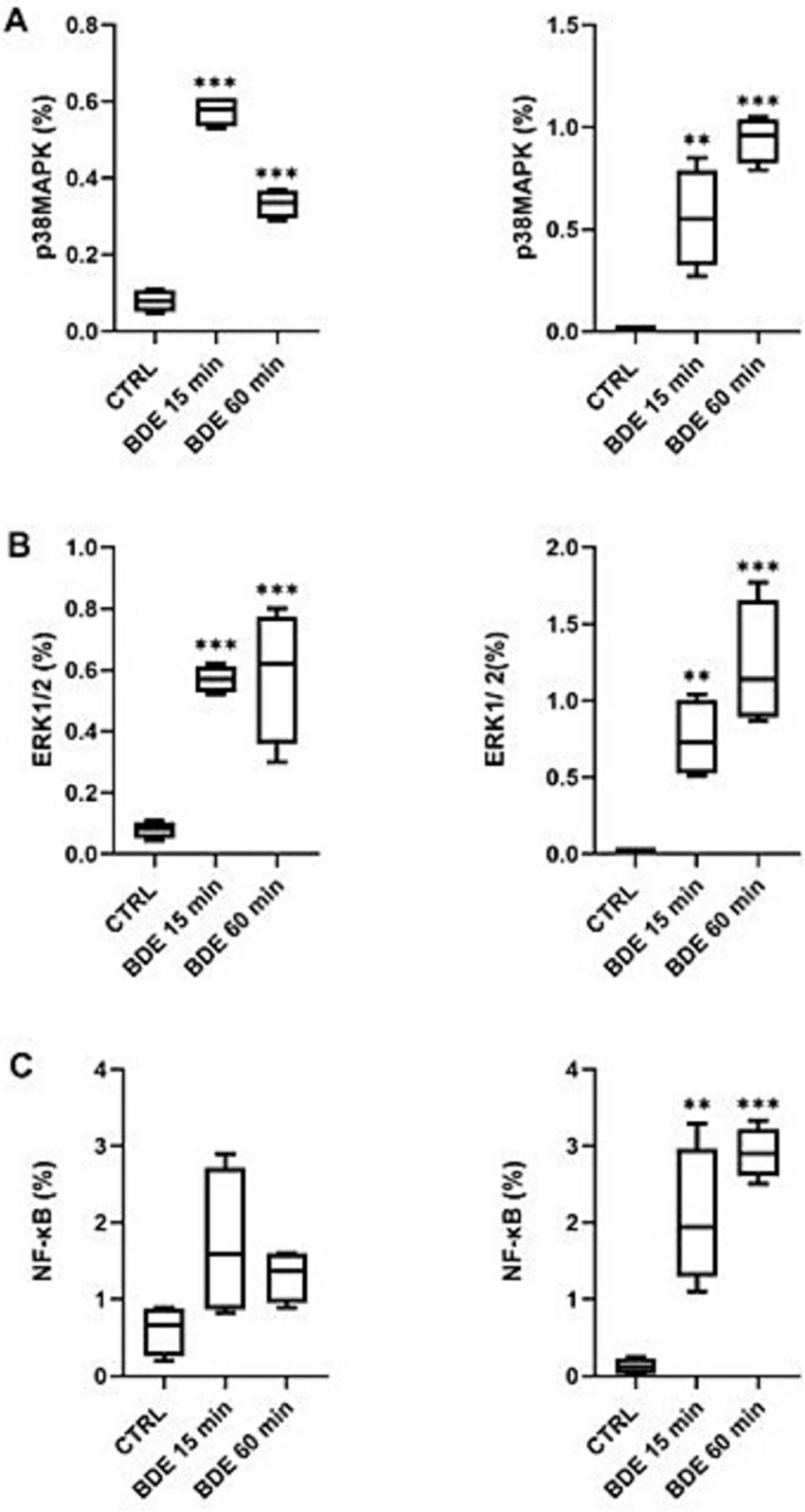

Figure 8. Activation percentage (%) of phospho-p38-MAPK (A), phospho-ERK1/2 (B) and phospho-NF-kB (p65) (C) by THP-1 cells incubated with RPMI 1640 (control—CTRL) or BDE (10 and 25 μg/ml, left and right respectively) for 15 and 60 min. $^{**}P < .01$; $^{***}P < .001$ vs CTRL (one-way ANOVA followed by post hoc Tukey test).

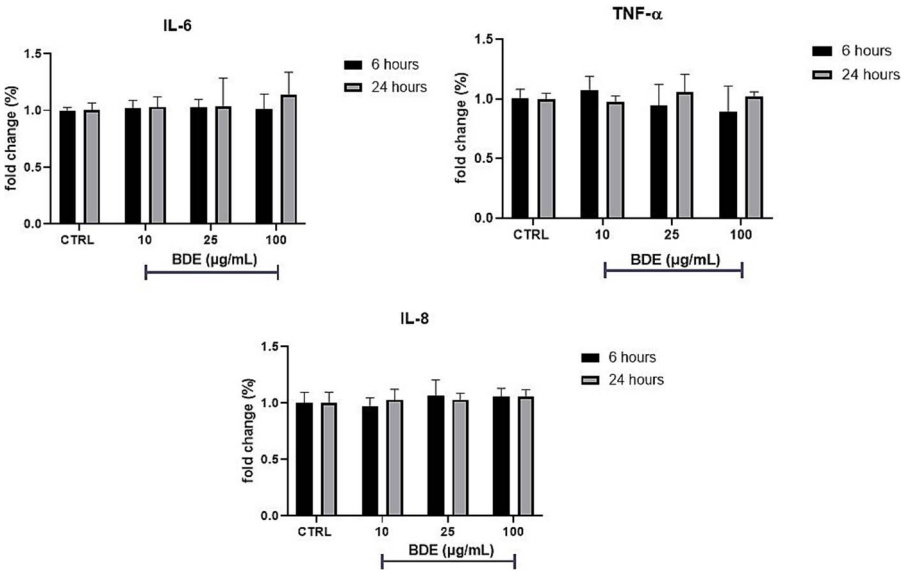

Figure 9. IL-6, TNF-α, and IL-8 production by THP-1 cells incubated with RPMI 1640 (control—CTRL) or with BDE (10, 25, and 100 μg/ml) for 6 and 24 h at basal conditions. Values were normalized to control and expressed as fold change ($P > .05$).

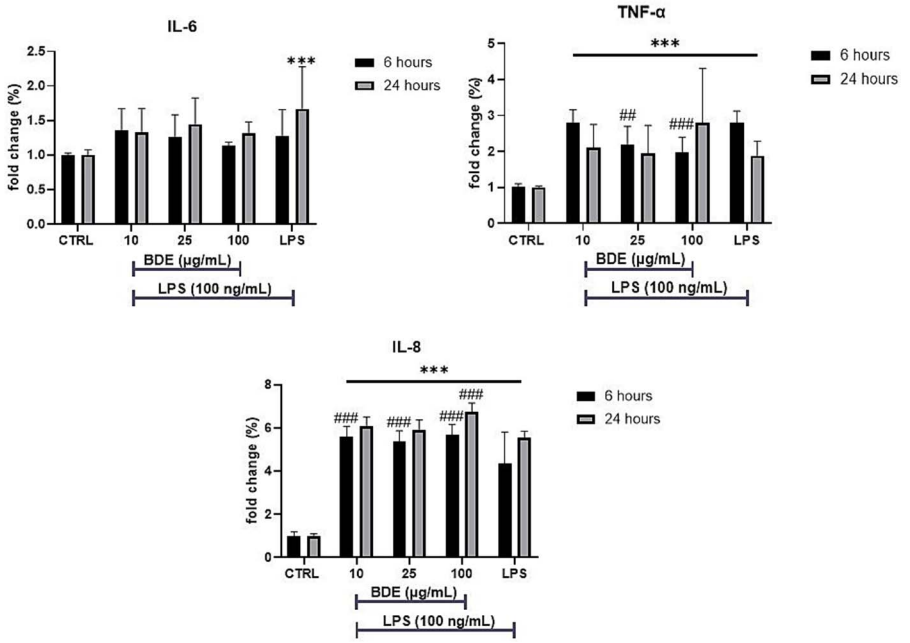

Figure 10. IL-6, TNF-α, and IL-8 production by THP-1 cells costimulated by BDE (10, 25 and 100 μg/ml) and LPS (100 ng/ml) for 6 and 24 h. Values were normalized to control and expressed as fold change. $^{***}P < .001$ vs ctrl; $^{\#\#}P < .01$; $^{\#\#\#}P < .001$ vs LPS (one-way ANOVA).

phytocomplex as a whole and to enhance its multitarget effects, rather than focusing exclusively on identifying the most promising single active compounds present in a complex plant matrix.

Simulated bioaccessibility tests showed that, among the molecules identified by HPLC-DAD, only pinocembrin exhibited good stability after digestive processes, around 80% ca.; when crossed with the boiled-egg model from *in silico* predictions, this result shows that pinocembrin is the most bioavailable molecule in the phytocomplex.

NP's predictions, which were performed using three different tools freely available, made possible to cross-reference the data obtained through UV–vis and HPLC-DAD analysis also implemented by database such as LOTUS and allow us obtain a pool of molecular targets that are likely to be used by BDE to carry out its biological activities. Using GeneRecommender's filters, the search could be directed towards molecular targets typical of the immune system, narrowing down its scope. Thus, NP enabled us to reduce experimental time and minimize research costs.

After establishing that there were no cytotoxic effects even at concentrations as high as 100 μg/ml, BDE was tested according to the data obtained from NP.

Aiming at investigating the molecular mechanisms underlying BDE biological activities, the involvement of TLR-2 and TLR-4 was initially evaluated by flow cytometry.

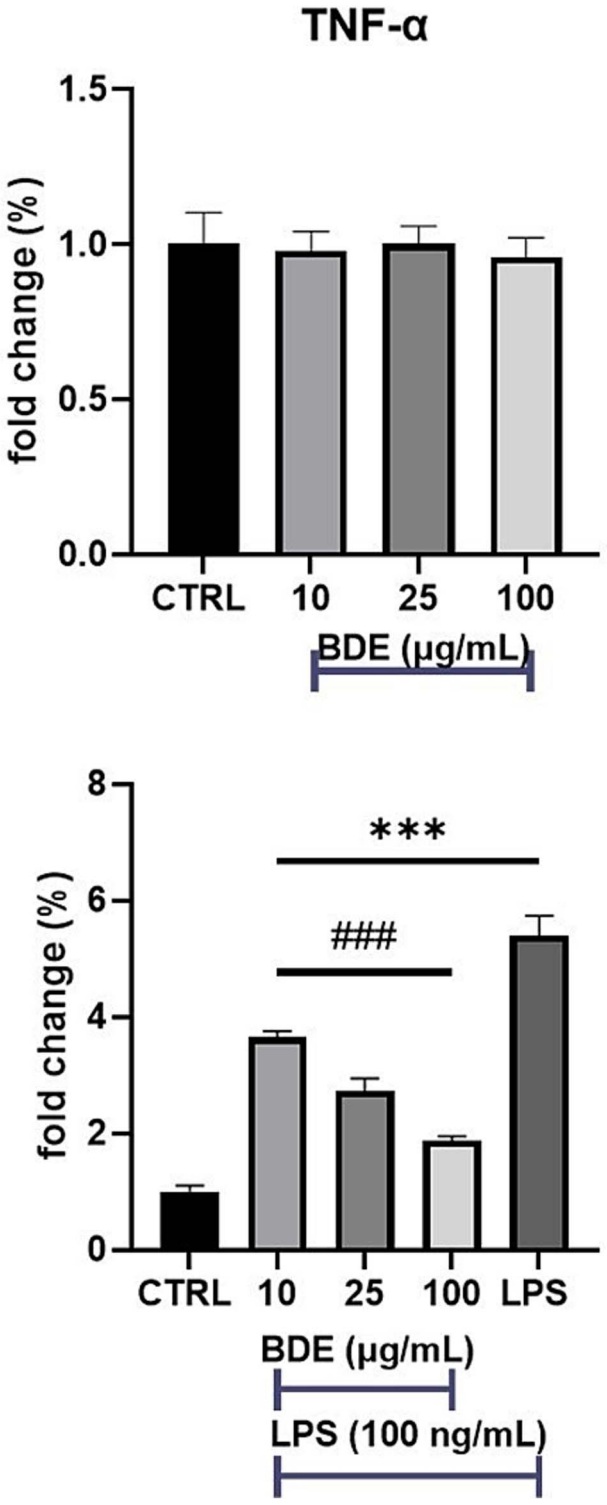

Figure 11. TNF-α production by THP-1 cells incubated with RPMI 1640 (control—CTRL) or with BDE (10, 25 and 100 μg/ml) for 2 h (above) or co-stimulated by BDE and LPS for 2 h (below). Values were normalized to control and expressed as fold change. $^{***}P < .001$ vs CTRL; $^{###}P < .001$ vs LPS (one-way ANOVA).

The information obtained from NP studies indicated the involvement of TLR-4 by BDE, a key receptor involved in innate immunity and the recognition of invading pathogens [25], a parameter confirmed by *in vitro* studies, through which its activation was confirmed. Although not predicted by computational studies, a slight nonsignificant increase in TLR-2 expression was observed. TLR-2 is a receptor typically found in immune cells that leads to the production of pro-inflammatory cytokines by activating intracellular signaling pathways such as NF-κB. Similarly, *in vitro* experiments confirmed the involvement of the three signaling pathways predicted by *in silico* analyses (ERK1/2, p38, and NF-κB), showing their significant activation induced by BDE even after 60 min.

Initial tests carried out on the THP-1 monocyte line under basal conditions showed that BDE was unable to increase the production of IL-6, TNF-α and IL-8 at any concentration. However, a slight decrease in TNF-α production was observed. Using LPS as a positive control in the inflammatory model and cotreating THP-1 cells with LPS and BDE led to interesting results: TNF-α production was inhibited after 2 and 6 h of treatment. There was also a slight reduction in IL-6 production after 24 h. Notably, BDE in combination with LPS increased IL-8 release after both 6 and 24 h, potentially promoting monocyte/macrophage recruitment to inflammatory or infectious sites [34].

Since BDE had an effect on THP-1 cells for a short period of time on TNF-α, which plays a fundamental role also in other immune cells and regulates the production of other cytokines [35], we decided to investigate BDE effects on a mixed cell population: PBMC. In human PBMC, BDE 25 mg/ml was able to positively and in a statistically significant manner modulate the production of IL-6, IL-2, IL-1β and IL-10 in basal conditions, suggesting the involvement of Th cells and, at the same time, validating NP predictions. Interestingly, at the same concentration, in LPS-stimulated PBMC, BDE reduced TNF-α and IL-10 in a significant manner. The specific upregulation of cytokines, which primarily involves those expressed by both monocytes and lymphocytes but does not include TNF-α, suggests that BDE could induce a post-transcriptional suppression of TNF-α, a cytokine known to be rapidly and specifically regulated, including via MAPK pathways. This hypothesis is further supported by the inhibitory effect on TNF-α expression in LPS-stimulated PBMC. The dual behavior of BDE in regulating IL-10, instead (upregulation in basal conditions and downregulation in LPS-stimulated cells), suggests that the extract could act upstream to modulate TLR-4 signaling. Importantly, our bioinformatic predictions guided us toward these targeted analyses and allowed us to propose subtle, nonobvious mechanisms that can be further investigated in future studies.

As regards the maximum tested concentration 100 μg/ml, even if recognized as nonphysiological, it provided interesting findings and confirmations, such as the additive effect with LPS in the production of IL-1β after 24 h, as well as that of IL-6 after 6 and 24 h, the dual activity of BDE on IL-10, the downregulation of IL-2 in LPS-stimulated cells and the maximum inhibitory effect on TNF-α production after 6 h, consistent with the THP-1 cell data, showing a concentration-dependent reduction in production, with BDE 100 μg/ml bringing levels back to baseline.

The immune activation found through the activation of TLR-2 and TLR-4 in particular, the involvement of the main immunological pathways and, at downstream level, cytokine modulation under both basal and inflammatory conditions, strengthened and confirmed the immunomodulatory activity

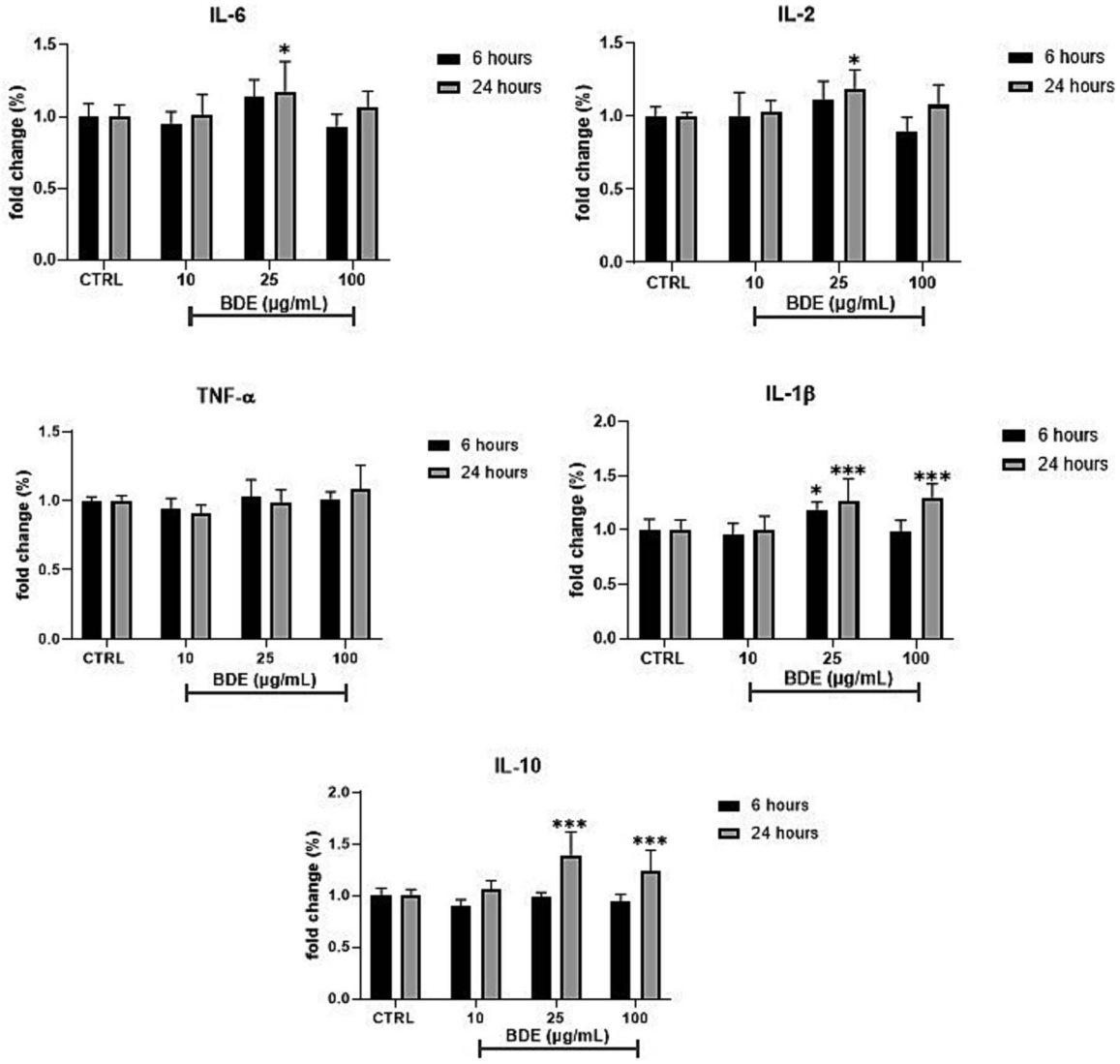

Figure 12. IL-6, IL-2, TNF-α, IL-1β and IL-10 production by PBMC incubated with RPMI 1640 (control—CTRL) or with BDE (10, 25 and 100 μg/ml) for 6 and 24 h at basal conditions. Values are normalized to control and expressed as fold change. $^{*}P < .05$; $^{***}P < .001$ vs CTRL (one-way ANOVA).

of *B. dracunculifolia* phytocomplex, not only when in Brazilian green propolis but also as native herbal matrix.

Within the field of medicinal plants with immunomodulatory effect, species such as *Echinacea purpurea* Moench., *E. pallida*, *E. angustifolia*, and *Pelargonium* sidoides DC. have been extensively studied and are officially recognized by the European Medicines Agency (EMA) for their use in the treatment and prevention of respiratory infections. These well-established examples highlight the typical multitarget approach of herbal medicinal products [36].

In this context, *B. dracunculifolia* emerges as a still underexplored yet promising resource. Its rich phytochemical profile, together with the findings presented in this study, suggest an immunomodulatory potential that warrants further investigation.

The integrated *in silico*/*in vitro* model was developed and validated on the basis that it could be improved further in the future, given potential technological developments. The first limitation certainly relates to the chemical analysis carried out using colorimetric and HPLC-DAD methods. These methods alone cannot provide a complete phytochemical characterization, although the LOTUS database has proven to be a valuable supporting tool in this regard. Secondly, the complexity of analysing the post-digested extracts by HPLC-DAD, which are characterised by numerous interferences due to the various components of the gastric and intestinal environments of the simulated digestion model, was highlighted. For this reason, future steps should focus on using more sophisticated equipment and models, such as LC-DAD-MS and high-resolution NMR, to better characterize the phytochemical profile of the different species studied. Alternatively, *in vitro* models, such as co-cultures or 3D models could be used, thus enabling faster translation of the results to the necessary *in vivo* experiments.

Regarding the investigated mechanism of action, we are aware that this work represents the first exploratory study valid to understand the biological potential of BDE, but using selective inhibitors, molecular probes or gene-silencing approaches we'll be able to provide more definitive insight into the mechanism involved.

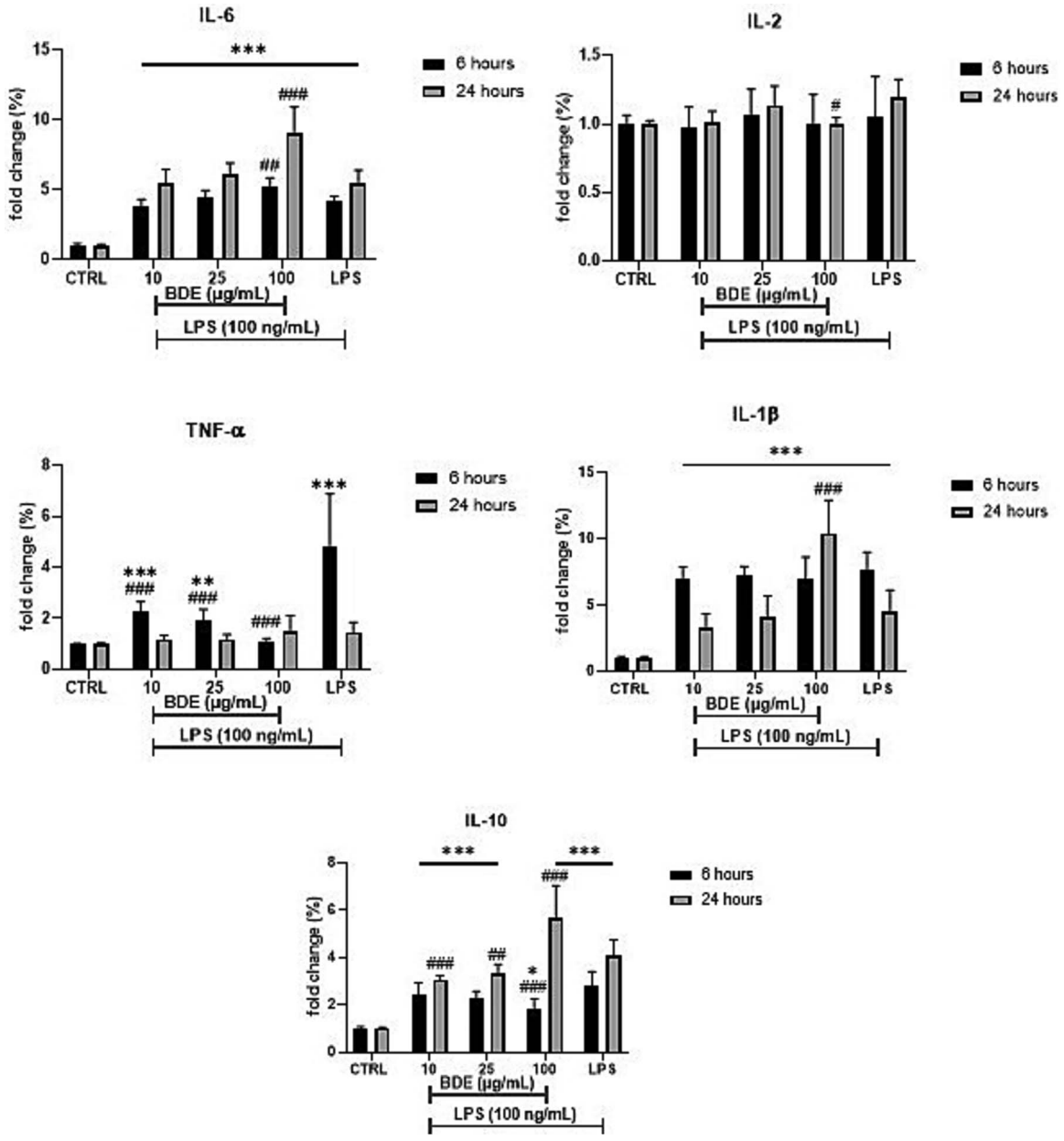

Figure 13. IL-6, IL-2, TNF-α, IL-1β, and IL-10 production by PBMC costimulated by BDE (10, 25, and 100 μg/ml) with LPS (100 ng/ml) for 6 and 24 h. Values were normalized to control and expressed as fold change. $^{*}P < .05$; $^{**}P < .01$; $^{***}P < .001$ vs CTRL; $^{\#}P < .01$; $^{\#\#}P < .01$; $^{\#\#\#}P < .001$ vs LPS (one-way ANOVA).

Further researches have been planned also to evaluate the action of BDE in animal models to observe its immunomodulatory effects *in vivo* with the aim of advancing towards clinical trials and technological development in the pharmaceutical sector.

Conclusion

NP approach using *in silico* methods enabled the *in vitro* analyses to be directed towards specific molecular targets. The results obtained, in most cases, allowed us both to verify and to confirm the information coming from the *in silico* analyses, but, above all, they have enabled us to validate the integrated *in silico/in vitro* model, demonstrating BDE immunomodulatory action.

B. dracunculifolia DC. is a species deeply rooted in South American traditional medicine and internationally known as the botanical source of Brazilian green propolis. Nevertheless, its phytocomplex as a whole remains largely unexplored from a scientific perspective. This study represents the first integrated effort to investigate the immunomodulatory potential of *B. dracunculifolia* through an integrated approach. The application of NP, supported by phytochemical analyses and biological validation, allowed for the identification of key molecular mechanisms involved in its activity, while simultaneously promoting an ethical and economically sustainable research model. Limitations and future perspectives overlap, as we consider it crucial to further explore both the phytochemical profile of BDE and the finer aspects of its immunomodulatory mechanism. In particular, future work

should address additional pathways suggested by the *in silico* analyses, including PI3K, downstream TLR adaptors such as TRIF, MAPK-related effectors such as MK2, and the NF-κB pathway, which remains a central hub in cytokine regulation. Overall, this study has successfully validated the proposed integrated *in silico/in vitro* model and demonstrated the immunomodulatory potential of *B. dracunculifolia*, providing a solid basis for its future valorization.

Acknowledgements

The authors are thankful to Prof. Dr Jairo Kenupp Bastos (FCFRP, USP, Brazil) for providing the BDE sample.

Author contributions

Giorgio Cappellucci: Validation, Visualization, Data curation, Investigation, Conceptualization, Methodology, Project administration, Writing—original draft. Marco Biagi: Validation, Visualization, Conceptualization, Methodology, Data curation. Mariana Romão-Veiga, Vanessa Rocha Ribeiro Vasques, Elisabetta Miraldi and Giulia Baini: Investigation, Data curation, Validation, Visualization. José Maurício Sforcin: Conceptualization, Supervision, Methodology, Validation, Writing—review & editing.

Supplementary data

Supplementary data is available at *Journal of Pharmacy and Pharmacology* online.

Conflict of interest

All authors declared that they have no potential conflict of interest.

Funding

None declared.

Data availability

Data available on request from the authors.

Ethical statement

This study was approved by the Ethics Committee of Botucatu Medical School, UNESP on April 09, 2024 (CAAE:78234224.8.0000.5411).

References

1. Neto BD, Medalha Colturato VM, Sicci Del Lama D *et al.* *Baccharis dracunculifolia* extract as a promising active for healing chronic wounds. *Int J Adv Med Biotechnol* 2023;**5**:2–7. https://doi.org/10.52466/ijamb.v5i2.114
2. Armstrong L, Raeski PA, Paes de Almeida V *et al.* Baccharis dracunculifolia DC. A review of research advances from 2004 to 2024, with new micromorphology and essential oil investigations. *J Herb Med* 2024;**48**:100952. https://doi.org/10.1016/j.hermed.2024.100952
3. Ritter MR, Christ Al, de Mello Zevieski A *et al.* An overview of the cultural and popular use of baccharis. In: Fernandes GW, Oki Y, Barbosa M, eds. Baccharis. Cham, Switzerland: Springer International Publishing 2021: 401–16. https://doi.org/10.1007/978-3-030-83511-8_16.
4. Gazim ZC, Valle JS, Carvalho dos Santos I *et al.* Ethnomedicinal, phytochemical and pharmacological investigations of *Baccharis dracunculifolia* DC. *(Asteraceae) Front Pharmacol* 2022;13. https://doi.org/10.3389/fphar.2022.1048688
5. Finetti F, Biagi M, Ercoli J *et al.* *Phaseolus vulgaris* L. var. venanzio grown in Tuscany: Chemical composition and *in vitro* investigation of potential effects on colorectal cancer. *Antioxidants (Basel)* 2020;**9**:1181. https://doi.org/10.3390/antiox9121181
6. Governa P, Cusi MG, Borgonetti V *et al.* Beyond the biological effect of a chemically characterized poplar propolis: Antibacterial and antiviral activity and comparison with flurbiprofen in cytokines release by LPS-stimulated human mononuclear cells. *Biomedicine* 2019;**7**:73. https://doi.org/10.3390/biomedicines7040073
7. Sberna G, Biagi M, Marafini G *et al.* *In vitro* evaluation of antiviral efficacy of a standardized hydroalcoholic extract of poplar type propolis against SARS-CoV-2. *Front Microbiol* 2022;13. https://doi.org/10.3389/fmicb.2022.799546
8. Cappellucci G, Paganelli A, Ceccarelli PL *et al.* Insights on the in vitro wound healing effects of *Sedum telephium* L. leaf juice. *Cosmetics* 2024b;**11**:131. https://doi.org/10.3390/cosmetics11040131
9. Monagas M, Gómez-Cordovés C, Bartolomé B *et al.* Monomeric, oligomeric, and polymeric flavan-3-ol composition of wines and grapes from *Vitis vinifera* L. cv. Graciano, Tempranillo, and cabernet sauvignon. *J Agric Food Chem* 2003;**51**:6475–81. https://doi.org/10.1021/jf030325+
10. Collodel G, Moretti E, Del Vecchio MT *et al.* Effect of chocolate and Propolfenol on rabbit spermatogenesis and sperm quality following bacterial lipopolysaccharide treatment. *Syst Biol Reprod Med* 2014;**60**:217–26. https://doi.org/10.3109/19396368.2014.911392
11. Pedrosa AM, de Castro WV, Castro AHF *et al.* Validated spectrophotometric method for quantification of total triterpenes in plant matrices. *DARU J Pharm Sci* 2020;**28**:281–6. https://doi.org/10.1007/s40199-020-00342-z
12. Rigillo G, Cappellucci G, Baini G *et al.* Comprehensive analysis of *Berberis aristata* DC. Bark extracts: *in vitro* and *in silico* evaluation of bioaccessibility and safety. *Nutrients* 2024;**16**:2953. https://doi.org/10.3390/nu16172953
13. Brodkorb A, Egger L, Alminger M *et al.* INFOGEST static *in vitro* simulation of gastrointestinal food digestion. *Nat Protoc* 2019;**14**:991–1014. https://doi.org/10.1038/s41596-018-0119-1
14. Rutz A, Sorokina M, Galgonek J *et al.* The LOTUS initiative for open knowledge management in natural products research. *elife* 2022;11. https://doi.org/10.7554/eLife.70780
15. Daina A, Michielin O, Zoete V. SwissTargetPrediction: Updated data and new features for efficient prediction of protein targets of small molecules. *Nucleic Acids Res* 2019;**47**:W357–64. https://doi.org/10.1093/nar/gkz382
16. Brambilla D, Giacomini DM, Muscarnera L *et al.* DeepProphet2 – A Deep Learning Gene Recommendation Engine. *arXiv*. 2022. https://doi.org/10.48550/arXiv.2208.01918
17. Szklarczyk D, Santos A, von Mering C *et al.* STITCH 5: Augmenting protein–chemical interaction networks with tissue and affinity data. *Nucleic Acids Res* 2016;**44**:D380–4. https://doi.org/10.1093/nar/gkv1277
18. Pressi G, Rigillo G, Governa P *et al.* A novel *Perilla frutescens* (L.) Britton cell-derived phytocomplex regulates keratinocytes inflammatory cascade and barrier function and preserves vaginal mucosal integrity *in vivo*. *Pharmaceutics* 2023;**15**:240. https://doi.org/10.3390/pharmaceutics15010240
19. Arvia R, Biagi M, Baini G *et al.* Ohba leaves juice improves herpetic lesions: New findings from *in vitro* investigations. *Nat Prod Res* 2024;1–9. https://doi.org/10.1080/14786419.2024.2423378
20. Pardo-Mora DP, Murillo OJ, Rey-Buitrago M *et al.* Apoptosis-related gene expression induced by Colombian propolis samples in canine osteosarcoma cell line. *Vet World* 2021;**14**:964–71. https://doi.org/10.14202/vetworld.2021.964-971

21. Gomes VJ, Nunes PR, Matias ML *et al.* Silibinin induces *in vitro* M2-like phenotype polarization in monocytes from preeclamptic women. *Int Immunopharmacol* 2020;**89**:107062. https://doi.org/10.1016/j.intimp.2020.107062
22. Matias ML, Gomes VJ, Romao-Veiga M *et al.* Silibinin downregulates the NF-κB pathway and NLRP1/NLRP3 inflammasomes in monocytes from pregnant women with preeclampsia. *Molecules* 2019;**24**:1548. https://doi.org/10.3390/molecules24081548
23. Iurckevicz G, Dahmer D, Casagrande M *et al.* Bioactive compounds in the leaves of *Baccharis dracunculifolia*: Extraction process and characterization. *Acta Sci Technol* 2021;**43**:e49826. https://doi.org/10.4025/actascitechnol.v43i1.49826
24. Bonin E, Carvalho VM, Avila VD *et al.* *Baccharis dracunculifolia*: Chemical constituents, cytotoxicity and antimicrobial activity. *LWT* 2020;**120**:108920. https://doi.org/10.1016/j.lwt.2019.108920
25. Skinner NA, Maclsaac CM, Hamilton JA *et al.* Regulation of toll-like receptor (TLR)2 and TLR4 on CD14dimCD16+ monocytes in response to sepsis-related antigens. *Clin Exp Immunol* 2005;**141**:270–8. https://doi.org/10.1111/j.1365-2249.2005.02839.x
26. Yang Y, Wang D, Li Q *et al.* Immune-enhancing activity of aqueous extracts from *Artemisia rupestris* L. via MAPK and NF-kB pathways of TLR4/TLR2 downstream in dendritic cells. *Vaccines (Basel)* 2020;**8**:525. https://doi.org/10.3390/vaccines8030525
27. Dalla Costa V, Piovan A, Filippini R *et al.* From ethnobotany to biotechnology: Wound healing and anti-inflammatory properties of *Sedum telephium* L. *in vitro* cultures. *Molecules* 2024;**29**:2472. https://doi.org/10.3390/molecules29112472
28. Sforcin JM, Biagi M. Effects of the green propolis on the immune response. In: Fernandes GW, Oki Y, Barbosa M, eds. Baccharis. Cham, Switzerland: Springer International Publishing 2021:535–46. https://doi.org/10.1007/978-3-030-83511-8_22.
29. Jin J, Chowdhury MHU, Das T *et al.* Chemico-biological interaction unraveled the potential mechanistic pathway of *Ixeridium dentatum* compounds against atopic dermatitis. *Comput Biol Chem* 2023;**106**:107933. https://doi.org/10.1016/j.compbiolchem.2023.107933
30. Adnan M, Jeon B-B, Chowdhury MHU *et al.* Network pharmacology study to reveal the potentiality of a methanol extract of *Caesalpinia sappan* L. wood against type-2 diabetes mellitus. *Life (Basel)* 2022;**12**:277. https://doi.org/10.3390/life12020277
31. Liao G, Yan Q, Zhang M *et al.* Integrative analysis of network pharmacology and proteomics reveal the protective effect of Xiaoqinglong decotion on neutrophilic asthma. *J Ethnopharmacol* 2024;**330**:118102. https://doi.org/10.1016/j.jep.2024.118102
32. Ding Z, Lu Y, Zhao J *et al.* Network pharmacology and molecular dynamics identified potential androgen receptor-targeted metabolites in *Crocus alatavicus*. *Int J Mol Sci* 2025;**26**:3533. https://doi.org/10.3390/ijms26083533
33. Deng Q, Chen W, Deng B *et al.* Based on network pharmacology, molecular docking and experimental verification to reveal the mechanism of *Andrographis paniculata* against solar dermatitis. *Phytomedicine* 2024;**135**:156025. https://doi.org/10.1016/j.phymed.2024.156025
34. Russell CD, Unger SA, Walton M *et al.* The human immune response to respiratory syncytial virus infection. *Clin Microbiol Rev* 2017;**30**:481–502. https://doi.org/10.1128/CMR.00090-16
35. Siegmund D, Wajant H. TNF and TNF receptors as therapeutic targets for rheumatic diseases and beyond. *Nat Rev Rheumatol* 2023;**19**:576–91. https://doi.org/10.1038/s41584-023-01002-7
36. Cappellucci G, Baini G, Miraldi E *et al.* Investigation on the efficacy of two food supplements containing a fixed combination of selected probiotics and β-glucans or elderberry extract for the immune system: Modulation on cytokines expression in human THP-1 and PBMC. *Foods* 2024a;**13**:458. https://doi.org/10.3390/foods13030458

Journal of Pharmacy and Pharmacology, 2025, 00, 1–16
https://doi.org/10.1093/jpp/rgaf110
Research Paper